



UNIVERSITY COLLEGE LONDON

MENG MECHANICAL ENGINEERING

MECH0074 EXTREME TEMPERATURE COURSEWORK

*Author:*

Hasha Dar

*Student number:*

19090799

*Module coordinator:*

Prof. Ian Eames

March 27, 2023

## Contents

<b>List of Figures</b>	<b>1</b>
<b>List of Tables</b>	<b>2</b>
<b>1 Influence of temperature on the response of a straight pipe</b>	<b>3</b>
1.1 Meaning and significance of stress terms . . . . .	3
1.1.1 Principal stress . . . . .	3
1.1.2 Von Mises stress . . . . .	4
1.1.3 Stress magnitude . . . . .	4
1.2 Relationship between axial stress and temperature of length constrained 3D pipe . . . . .	4
1.3 3D pipe ANSYS . . . . .	6
1.3.1 Relationship between maximum stress in temperature range . . . . .	6
1.3.2 Comparison against theoretical result and discussion . . . . .	8
1.4 1D pipe ANSYS . . . . .	9
1.4.1 Relationship between maximum stress in temperature range . . . . .	9
1.4.2 Comparison against theoretical result and discussion . . . . .	12
1.5 Discussion . . . . .	13
1.5.1 Difference and similarities between results from 1.2, 1.3, 1.4 as pipe slenderness changes .	13
1.5.2 Model errors encountered using ANSYS Static Structural model . . . . .	14
<b>2 Influence of temperature on the response of an expansion loop</b>	<b>14</b>
2.1 Comparison of shape of expansion loop . . . . .	14
2.2 Plot of variation of maximum displacement of pipe bends . . . . .	16
2.3 Plot of variation of maximum stress of pipe bends . . . . .	18
2.4 Comparison of numerical results . . . . .	19
2.5 1D pipe model and consequences of increasing length L1 and effect on maximum pipe stress .	21
<b>References</b>	<b>24</b>
<b>A Code for Part 1C</b>	<b>25</b>
<b>B Code for Part 1D</b>	<b>26</b>
<b>C Code for Part 2B</b>	<b>27</b>
<b>D Code for Part 2C</b>	<b>28</b>
<b>E Code for Part 2E</b>	<b>29</b>

## List of Figures

1 Geometry of 3D pipe with probe region in the centre. . . . .	6
2 Setup for remote displacement applied on the surface of both ends of 3D pipe. . . . .	7
3 Plot of $\sigma_m$ in 3D pipe. . . . .	7
4 3D pipe at time-step 21, 240 °C, axial stress. . . . .	8
5 3D pipe at time-step 21, 240 °C, deformation. Note that the inside of the pipe has expanded less than the outside, i.e. the thickness of the pipe changes. . . . .	8
6 Plot of $\sigma_m$ in 3D pipe from ANSYS and theoretical calculation. . . . .	9
7 Geometry of 1D pipe with probe region in the centre. Mesh view was chosen for visualisation purposes. . . . .	10
8 Setup for fixed supports applied on the ends of the pipe and thermal condition. . . . .	10
9 Plot of $\sigma_m$ in 1D pipe. . . . .	11
10 1D pipe at time-step 21, 240 °C, axial stress. . . . .	11

11	1D pipe at time-step 21, 240 °C, deformation. Note that there is no deformation. . . . .	12
12	Plot of $\sigma_m$ in 1D pipe from ANSYS and theoretical calculation. . . . .	12
13	3D expansion loop geometry. . . . .	14
14	3D expansion loop deformation in comparison to undeformed case at $T = -160$ °C. . . . .	15
15	3D expansion loop deformation in comparison to undeformed case at $T = 240$ °C. . . . .	15
16	ANSYS maximum deformation in x-axis at time step 21, $T - T_0 = 218$ °C, bottom pipe bend.	16
17	ANSYS maximum deformation in y-axis at time step 21, $T - T_0 = 218$ °C, bottom pipe bend.	16
18	ANSYS maximum deformation in x-axis at time step 1 and 21, $T - T_0 = -188$ °C – 218 °C, bottom pipe bend. . . . .	17
19	Node selected for pipe bend analysis. . . . .	17
20	Plot to show maximum displacement of bottom pipe bend at node of maximum displacement.	17
21	Plot to show maximum displacement of top pipe bend at node of maximum displacement. . . . .	18
22	ANSYS maximum principal stress contour plot at time step 21, $T - T_0 = 218$ °C, bottom pipe bend. . . . .	18
23	Plot to show maximum principal stress $\sigma_1$ of pipe bends. . . . .	19
24	Plot to show maximum principal and shear stress of pipe bends. . . . .	19
25	ANSYS results from 1D expansion loop $L_1 = 10$ m, time step 1, $T = -160$ °C, maximum combined stress. . . . .	21
26	ANSYS results from 1D expansion loop $L_1 = 10$ m, time step 21, $T = 240$ °C, maximum combined stress. . . . .	21
27	ANSYS results from 1D expansion loop $L_1 = 50$ m, time step 1, $T = -160$ °C, maximum combined stress. . . . .	22
28	ANSYS results from 1D expansion loop $L_1 = 50$ m, time step 21, $T = 240$ °C, maximum combined stress. . . . .	22
29	Maximum combined stress of $L_1$ 50 m and 10 m expansion loops. . . . .	23

## List of Tables

1	Values of variables used for theoretical calculation of 3D pipe stress. . . . .	8
---	---	---

# 1 Influence of temperature on the response of a straight pipe

## 1.1 Meaning and significance of stress terms

### 1.1.1 Principal stress

Principal stress is a measure which defines the maximum normal stress which may be applied to a body of interest and where that stress is located. In the 3D case, we find that there exist three principal planes (where the shear stress is zero), which are orthogonal and each have their own maximum / minimum normal stresses. From this, we can also find locations and magnitude for the maximum shear stress.

Consider the six components of the 3D solid stress tensor:

$$\sigma_{ij} = \begin{bmatrix} \sigma_x & \tau_{yx} & \tau_{zx} \\ \tau_{xy} & \sigma_y & \tau_{zy} \\ \tau_{xz} & \tau_{yz} & \sigma_z \end{bmatrix} \quad (1)$$

where the first subscript denotes the direction of the surface normal and the second the direction of the stress. For static equilibrium:

$$\tau_{xy} = \tau_{yx} \quad \tau_{xz} = \tau_{zx} \quad \tau_{zy} = \tau_{yz} \quad (2)$$

By rotating the coordinate axes of our 3D body, we can change the components of the solid stress tensor, whilst representing the same state of stress on the body. As our matrix is symmetric, we can calculate a set of orthogonal axes which result in all  $\tau$  elements equalling zero. This set of axes is called the principal axes and by applying this transformation to our solid stress tensor, we find the eigenvalues of the matrix and the principal stresses. Hence:

$$\sigma_{ij} = \begin{bmatrix} \sigma_x & \tau_{yx} & \tau_{zx} \\ \tau_{xy} & \sigma_y & \tau_{zy} \\ \tau_{xz} & \tau_{yz} & \sigma_z \end{bmatrix} \xrightarrow{\text{eigenvalues}} \sigma'_{ij} = \begin{bmatrix} \sigma_1 & 0 & 0 \\ 0 & \sigma_2 & 0 \\ 0 & 0 & \sigma_3 \end{bmatrix} \quad (3)$$

$$\det(\sigma - \sigma I) = 0 \quad (4)$$

where  $I$  is the identity matrix and  $\sigma$  is the eigenvalue. The eigenvectors of the stress tensor, which correspond to the principal directions (the angles between the original (or base) coordinate axes and the new (or transformed) coordinate axes), can be found by solving the equation:

$$(\sigma - \sigma I)v = \mathbf{0} \quad (5)$$

where  $v$  is the eigenvector. This may also be written as:

$$\cos \alpha = \cos(n, x) = l \quad (6)$$

$$\cos \beta = \cos(n, y) = m \quad (7)$$

$$\cos \gamma = \cos(n, z) = n \quad (8)$$

where  $n$  is the unit normal to the plane. We can now define the normal stress acting on any oblique plane:

$$\sigma_{x'} = \sigma_x l^2 + \sigma_y m^2 + \sigma_z n^2 + 2(\tau_{xy}lm + \tau_{xy}mn + \tau_{xz}ln) \quad (9)$$

We are interested in the maximum and / or minimum values of the normal stress acting on our body throughout the range of oblique planes. These maxima / minima are the principal stresses. This is determined by calculating the differentials of the above equations with respect to the direction cosines. We find that the principal stresses occur on planes where the shear stress is zero, as mentioned previously. The equations for in-plane principal stresses are shown below. The third stress is zero in plane stress conditions.

$$\sigma_1 = \left( \frac{\sigma_x + \sigma_y}{2} \right) + \sqrt{\left( \frac{\sigma_x - \sigma_y}{2} \right)^2 + \tau_{xy}^2} \quad (10)$$

$$\sigma_2 = \left( \frac{\sigma_x + \sigma_y}{2} \right) - \sqrt{\left( \frac{\sigma_x - \sigma_y}{2} \right)^2 + \tau_{xy}^2} \quad (11)$$

A key characterisation of the principal stress is that it acts in the normal direction to the principal plane - this is important to note as a distinction. The determination of the principal stresses (and maximum shear stress) is important for design purposes as it tells us whether a body would be able to withstand a design load at a given location.

### 1.1.2 Von Mises stress

Von Mises stress can be used to determine whether an isotropic and ductile material will yield under a complex loading condition. The von Mises stress equation is based on the principle that the failure of a material is dependent on the total amount of energy that is being absorbed by the material, rather than the individual stresses in each direction. The equation simplifies the complex stress state of a material, which is often composed of multiple stresses acting in different directions, into a single numerical value that is used to determine whether the material is likely to fail. A comparison between the material's yield stress and the von Mises stress allows the calculation of the von Mises Stress Criterion.

An equation for the von Mises stress is shown below.

$$\sigma_{VM} = \sqrt{\frac{1}{2} [(\sigma_x - \sigma_y)^2 + (\sigma_y - \sigma_z)^2 + (\sigma_z - \sigma_x)^2] + 3 (\tau_{xy}^2 + \tau_{yz}^2 + \tau_{zx}^2)} \quad (12)$$

However, we can also calculate the von Mises stress directly from the principal stresses (note that we may not do the reverse).

$$\sigma_{VM} = \sqrt{\frac{1}{2} [(\sigma_1 - \sigma_2)^2 + (\sigma_2 - \sigma_3)^2 + (\sigma_3 - \sigma_1)^2]} \quad (13)$$

The von Mises stress is often used in engineering design to determine whether a material will fail under a given load. If the von Mises stress exceeds the yield strength of the material, plastic deformation is expected to occur. Therefore, designers can use the von Mises stress to ensure that their designs remain within the elastic limit of the material.

### 1.1.3 Stress magnitude

Stress magnitude refers to the amount or level of stress experienced by an object or system. Stress, in essence, describes the force per unit area acting on a material, and stress magnitude is determined by the magnitude of this force.

## 1.2 Relationship between axial stress and temperature of length constrained 3D pipe

The derivation presented here concerns the thermal bowing of a laterally restrained beam or pipe subjected to a uniform temperature gradient. The derivation aims to obtain an equation that describes the lateral displacement of the beam due to the thermal load.

The starting point of the derivation is the expression for the displacement of a point in the beam. The displacement can be expressed as a function of the position along the beam,  $x$ , and two lateral coordinates,  $y$  and  $z$ , as:

$$u(x, y, z) = f(x) + yf_1(x) + zf_2(x) \quad (14)$$

where  $f(x)$  is the longitudinal displacement,  $f_1(x)$  is the lateral slope, and  $f_2(x)$  is the curvature.

The longitudinal strain in the beam can be expressed as the partial derivative of the displacement with respect to the longitudinal coordinate,  $x$ , as:

$$\epsilon_{xx} = \frac{\partial u}{\partial x} = f'(x) + yf'_1(x) + zf'_2(x) \quad (15)$$

The stress field in the beam can be expressed as a function of the longitudinal strain and the temperature distribution in the beam. Assuming that the temperature distribution is uniform and the longitudinal strain is solely due to thermal expansion, the stress field can be expressed as:

$$\sigma_{xx} = E (\epsilon_{xx} - \alpha T) \quad (16)$$

where  $E$  is the modulus of elasticity of the material,  $\alpha$  is the coefficient of thermal expansion, and  $T$  is the temperature in the beam.

The equilibrium of forces and moments in the beam requires that the stress field integrates to zero over the cross-sectional area of the beam. Assuming that the temperature distribution is uniform, this condition can be expressed as:

$$\int \sigma_{xx} dA = 0 \quad (17)$$

$$\int \sigma_{xy} dA = 0 \quad (18)$$

$$\int \sigma_{xz} dA = 0 \quad (19)$$

where  $dA$  is an element of the cross-sectional area of the beam, and  $y$  and  $z$  are the lateral coordinates of the element.

The geometrical constraint is that the center of gravity of the cross-pipe must be located at the origin:

$$\int y dA = \int z dA = 0 \quad (20)$$

Next, we consider the cross-pipe variation of temperature. The stress field in x-direction can be expressed as:

$$\sigma_{xx} = -\alpha E (T - T_0) + \frac{I_y M_{Tz} - I_{yz} M_{Ty}}{I_y I_z - I_{yz}^2} y + \frac{I_y M_{Tz} - I_{yz} M_{Ty}}{I_y I_z - I_{yz}^2} z \quad (21)$$

where  $T$  is the temperature at any given point, and  $T_0$  is the average temperature of the pipe.  $I_z$ ,  $I_y$  and  $I_{yz}$  are the moments of inertia of the cross-sectional area with respect to yz, zx and xy planes respectively.  $M_{Ty}$  and  $M_{Tz}$  are the moments due to the variation of temperature.

For a pipe with a circular cross-section,  $I_z$  and  $I_y$  are equal, and  $I_{yz}$  is zero. Hence, the stress field in the x-direction reduces to:

$$\sigma_{xx} = -\alpha E (T - T_0) + \frac{M_{Tz}}{I_y} y \quad (22)$$

We can now derive the equation for lateral displacement of the pipe. The lateral displacement is obtained by taking the second derivative of the displacement function with respect to  $x$ :

$$\frac{d^2 v}{dx^2} = -\frac{M_{Tz}}{EI_z} \quad (23)$$

$$\frac{d}{dx^2} \left( EI_z \frac{d^2 v}{dx^2} \right) + \frac{d^2 M_{Tz}}{dx^2} = F \quad (24)$$

The tensile force  $P$  and a tensile  $P - \delta$  moment  $Py$  over the length of the beam give us the equation governing the displacement of the beam:

$$\frac{d^2 y}{dx^2} = \phi + \frac{Py}{EI} \quad (25)$$

where  $y(x)$  is the displacement of the beam at position  $x$ ,  $\phi$  is the lateral displacement due to the uniform thermal gradient,  $E$  is the Young's modulus,  $I$  is the second moment of area.

Using the expression for the moment,  $M = EI\phi = EI\alpha T_{,y}$ , where  $\alpha$  is the coefficient of thermal expansion and  $T_{,y}$  is the temperature gradient, we can obtain the value of  $P$  as:

$$P = \frac{EI\alpha T_{,y}}{y} \quad (26)$$

Substituting this expression for  $P$  into the equation for the displacement, we get:

$$\frac{d^2 y}{dx^2} - k^2 y = \phi \quad (27)$$

where  $k = \sqrt{P/EI}$ . The solution to this differential equation is given by:

$$y(x) = -\frac{\phi}{k^2} \left( \frac{\cosh(kl) - 1}{\sinh(kl)} \sinh(kx) \cosh(kx) + 1 \right) \quad (28)$$

where  $l$  is the length of the beam. This equation gives the displacement of the beam at any point  $x$  due to the uniform thermal gradient, and it shows that the maximum displacement occurs at the mid-span of the beam, where

$$y(l/2) = \frac{\phi}{k^2 \tanh(kl/2)} \quad (29)$$

Some approximations and limitations in this analysis come from the constraints used in this application. Usmani *et al* outline that assuming that the axial restraints being perfectly rigid is practically impossible. Hence, an approach using axial restraints modelled with a spring with stiffness  $k_s$  are more likely to be observed in real-world beams [1].

## 1.3 3D pipe ANSYS

### 1.3.1 Relationship between maximum stress in temperature range

ANSYS was used to conduct analysis on a 3D pipe to determine the relationship between maximum stress  $\sigma_m$  and  $T - T_0$  over the temperature range specified as  $T = -160^\circ\text{C}$  and  $T = 240^\circ\text{C}$  with  $T_0 = 22^\circ\text{C}$ . The pipe external and internal diameters and length were specified as  $D_e = 813 \text{ mm}$ ,  $D_i = 793.94 \text{ mm}$  and  $L = 50 \text{ m}$ .

The geometry was constructed using ANSYS Discovery, and a test region of  $\pm 2.5 \text{ m}$  from the centre of the pipe was chosen to probe the results. The setup is shown in Figure 1

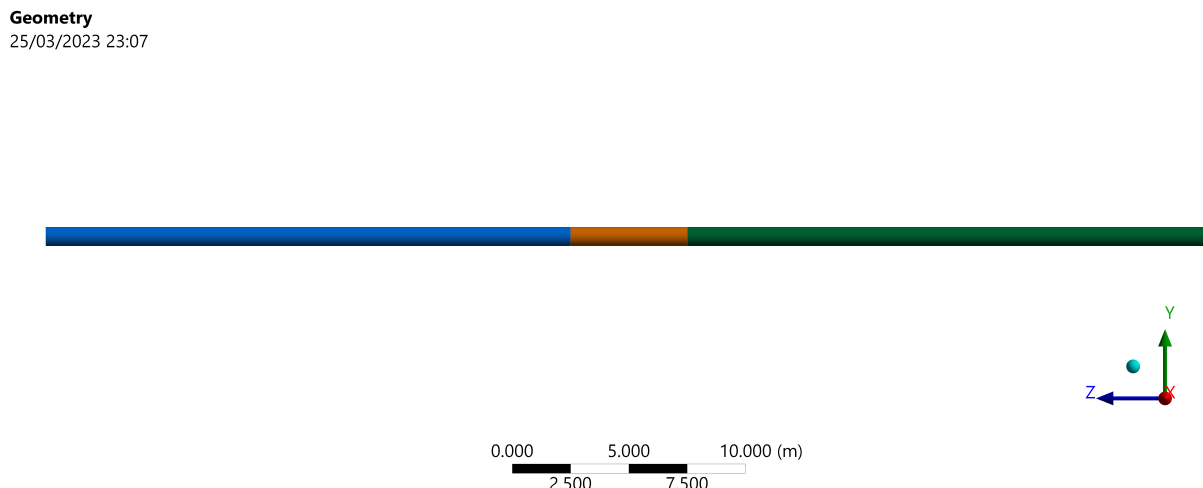


Figure 1: Geometry of 3D pipe with probe region in the centre.

The constraints used in the analysis were carefully chosen to ensure that the resulting simulation was accurate. The use of ‘remote displacements’ proved to provide the best representation of the support required for this analysis. These remote displacements were fixed in all axes and rotations. They were applied on the surfaces of both ends of the pipe. The remote point was chosen as the geometric centre of the pipe in the same plane (x-y). The support setup is shown in Figure 2.

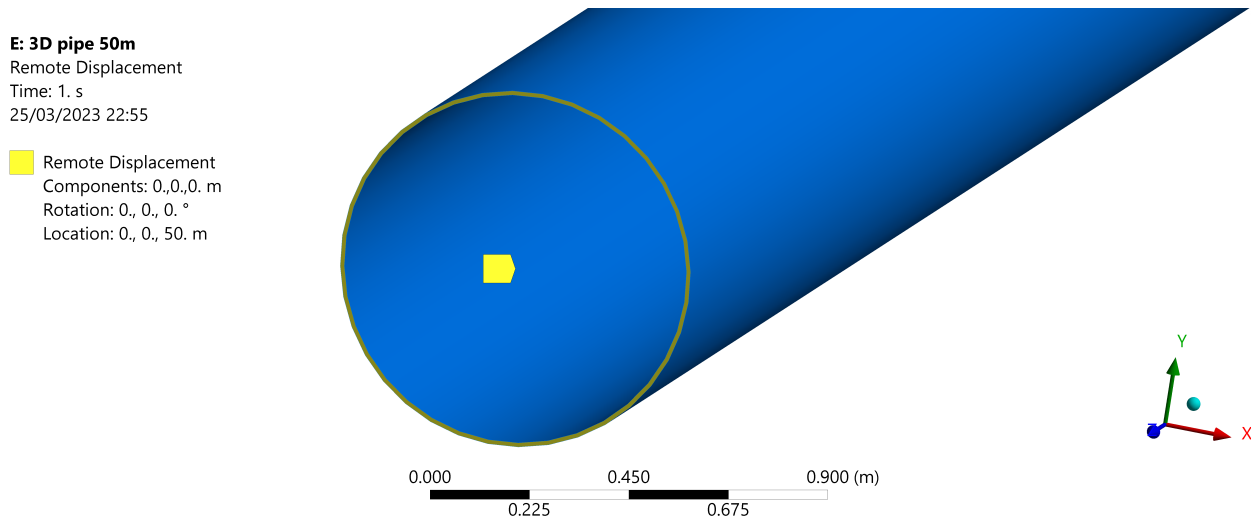


Figure 2: Setup for remote displacement applied on the surface of both ends of 3D pipe.

Using fixed supports gave results with abnormal edge cases. ANSYS documentation has noted this issue with fixed supports applied on surfaces, edges and vertices. Fixed supports lead to singular stresses i.e. the stress approaches infinity near the fixed edge or vertex [2]. Another problem with fixed surfaces is the non-compliance in deformation in the x-y plane. We expect to see the pipe expand/contract in this plane due to thermal effects. Running the simulation with fixed supports showed that the main body of the pipe does expand and contract but the elements connected to the fixed surface at the ends of the pipe do not, leading to an abnormalities.

In comparison, remote displacements allowed the ends of the pipe to expand/contract in the x-y plane, but did not allow the pipe to move in the z-axis. This manifests in a variation in the stress at the ends of the pipe. This variation is relatively small, with variation of around 1% from the average. As we are probing results from the centre of the pipe, this can be excluded from our discussion. A thermal condition was applied to the geometry spanning  $-160^{\circ}\text{C}$  to  $240^{\circ}\text{C}$ .

To determine the maximum stress  $\sigma_m$ , ‘Normal stress’ was indexed in the solution. This was configured to determine the maximum normal stress in the z-axis. The simulation utilised 21 steps, resulting in linear temperature steps of  $20^{\circ}\text{C}$ . The results are shown in Figures 3, 4, 5.

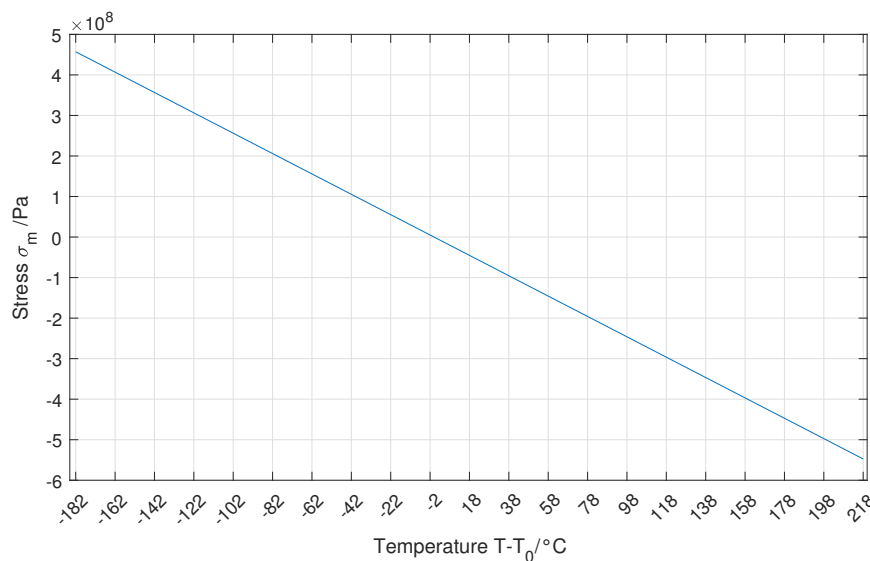


Figure 3: Plot of  $\sigma_m$  in 3D pipe.

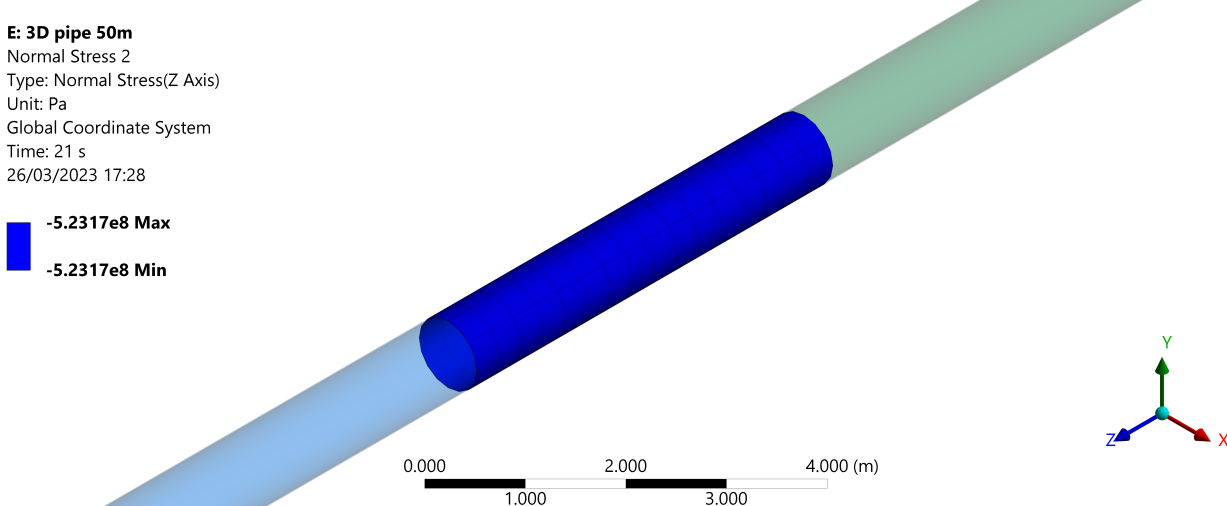


Figure 4: 3D pipe at time-step 21, 240 °C, axial stress.

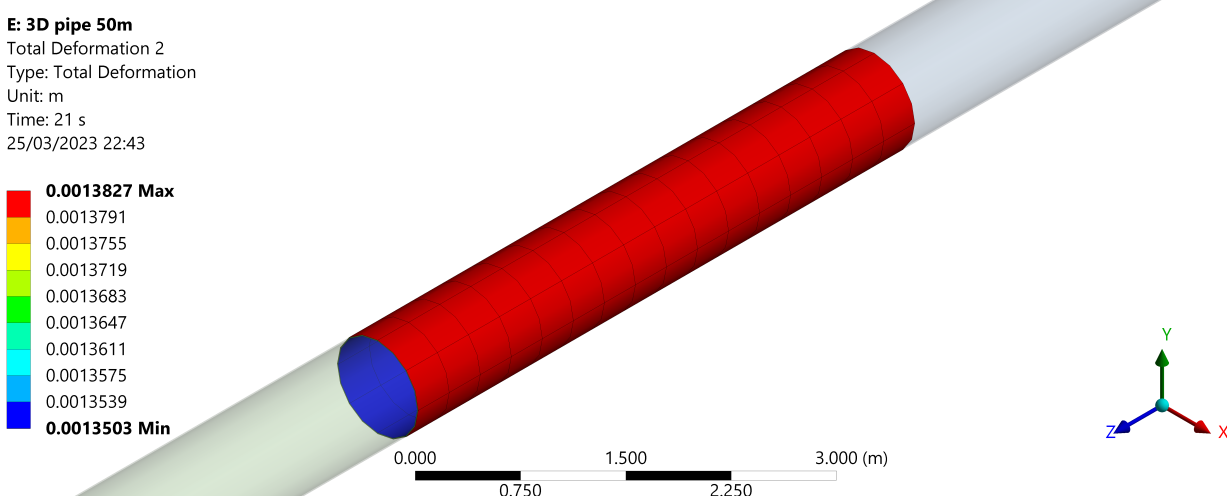


Figure 5: 3D pipe at time-step 21, 240 °C, deformation. Note that the inside of the pipe has expanded less than the outside, i.e. the thickness of the pipe changes.

### 1.3.2 Comparison against theoretical result and discussion

The theoretical result was calculated using (30). MATLAB was used to plot the results. Figure 6 shows the results from ANSYS and MATLAB plotted on the same graph. The variables used in the equation are shown in Table 1. The value of  $M_{Tz}$  was set to zero in this case, as the bending moment is zero (from constraints).

$$\sigma_{xx} = -\alpha E (T - T_0) + \frac{M_{Tz}}{I_y} y \quad (30)$$

Variable	Value	Source
$\alpha$	$1.2 \times 10^{-5} \text{ }^{\circ}\text{C}^{-1}$	ANSYS Engineering Data
$E$	$2 \times 10^{11} \text{ Pa}$	ANSYS Engineering Data
$T_0$	22 °C	User-defined

Table 1: Values of variables used for theoretical calculation of 3D pipe stress.

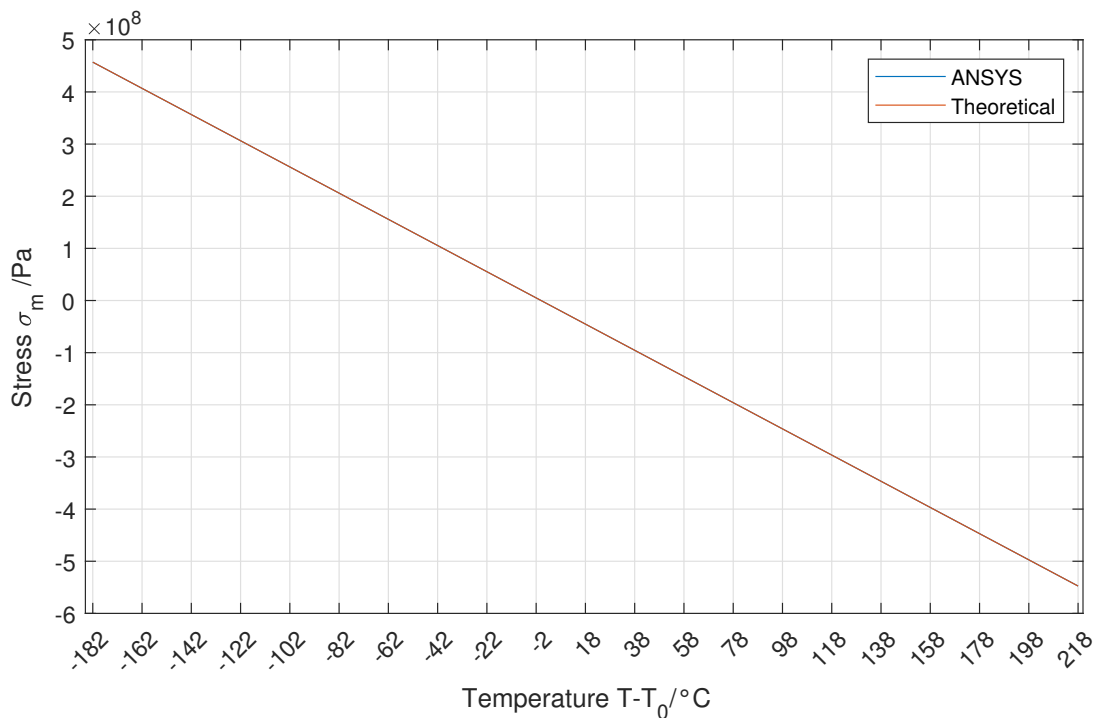


Figure 6: Plot of  $\sigma_m$  in 3D pipe from ANSYS and theoretical calculation.

The results show a virtually identical stress magnitude. An average percentage of difference of  $6.12 \times 10^{-5} \%$  was calculated for the results. The material properties were copied from ANSYS itself, and hence can be ruled out as a source of inaccuracy. The boundary conditions described above are the same between ANSYS and theoretical and can also be ruled out.

The slight difference in the numerical and theoretical results may arise from the numerical methods that ANSYS uses to solve the equations that describe the system. As noted previously, we see a very slight change in the thickness of the pipe, as the temperature varies and this could be contributing a small amount to the axial stress.

## 1.4 1D pipe ANSYS

### 1.4.1 Relationship between maximum stress in temperature range

ANSYS was used to conduct analysis on a 1D pipe to determine the relationship between maximum stress  $\sigma_m$  and  $T - T_0$  over the temperature range specified as  $T = -160 {}^\circ\text{C}$  and  $T = 240 {}^\circ\text{C}$  with  $T_0 = 22 {}^\circ\text{C}$ . The pipe external and internal diameters and length were specified as  $D_e = 813 \text{ mm}$ ,  $D_i = 793.94 \text{ mm}$  and  $L = 50 \text{ m}$ .

The geometry was constructed using ANSYS SpaceClaim, and a test region of  $\pm 2.5 \text{ m}$  from the centre of the pipe was chosen to probe the results. The setup is shown in Figure 7

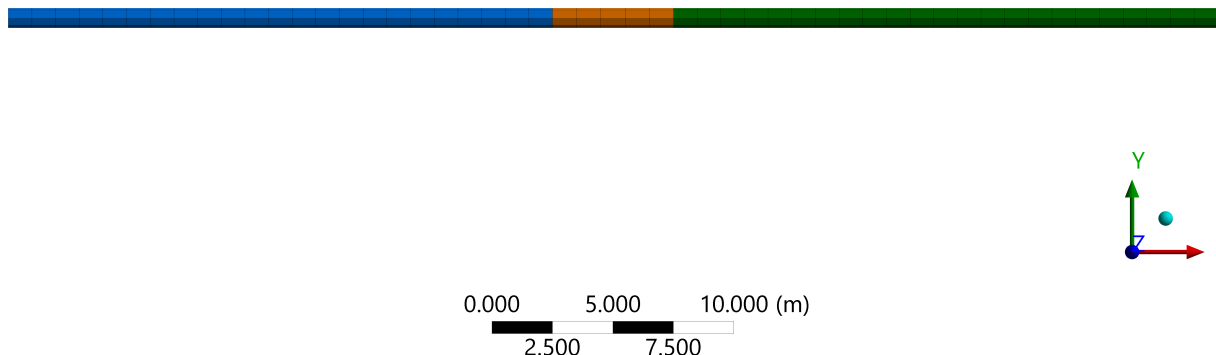


Figure 7: Geometry of 1D pipe with probe region in the centre. Mesh view was chosen for visualisation purposes.

'Fixed supports' were utilised at the ends of the pipe, to fix the displacement and rotation of the pipe in and around all axes. As the beam is modelled as a line segment with a given cross-section in 1D, there is no need to use a remote displacement to specify a particular constraint/behaviour in the x-y plane for the geometry. Two joint connections were also applied between each line segment to connect the geometry together. A thermal condition was applied to the geometry spanning  $-160\text{ }^{\circ}\text{C}$  to  $240\text{ }^{\circ}\text{C}$ . The setup is shown in Figure 8.

**B: 1D pipe 50m**  
 Static Structural  
 Time: 1. s  
 26/03/2023 16:50

**A** Fixed Support  
**B** Fixed Support 2  
**C** Thermal Condition:  $-160\text{ }^{\circ}\text{C}$

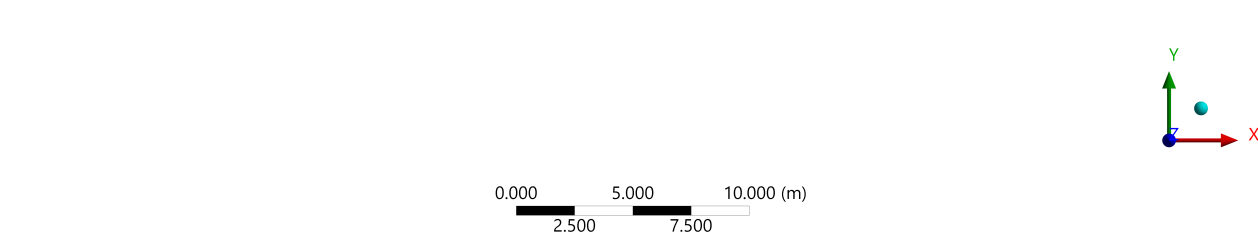


Figure 8: Setup for fixed supports applied on the ends of the pipe and thermal condition.

To determine the maximum stress  $\sigma_m$ , 'Beam tool' was indexed in the solution. This was configured to determine the maximum normal stress in the z-axis using the 'Direct stress' tool. The simulation utilised 21 steps, resulting in linear temperature steps of  $20\text{ }^{\circ}\text{C}$ . The results are shown in Figures 9, 10, 11.

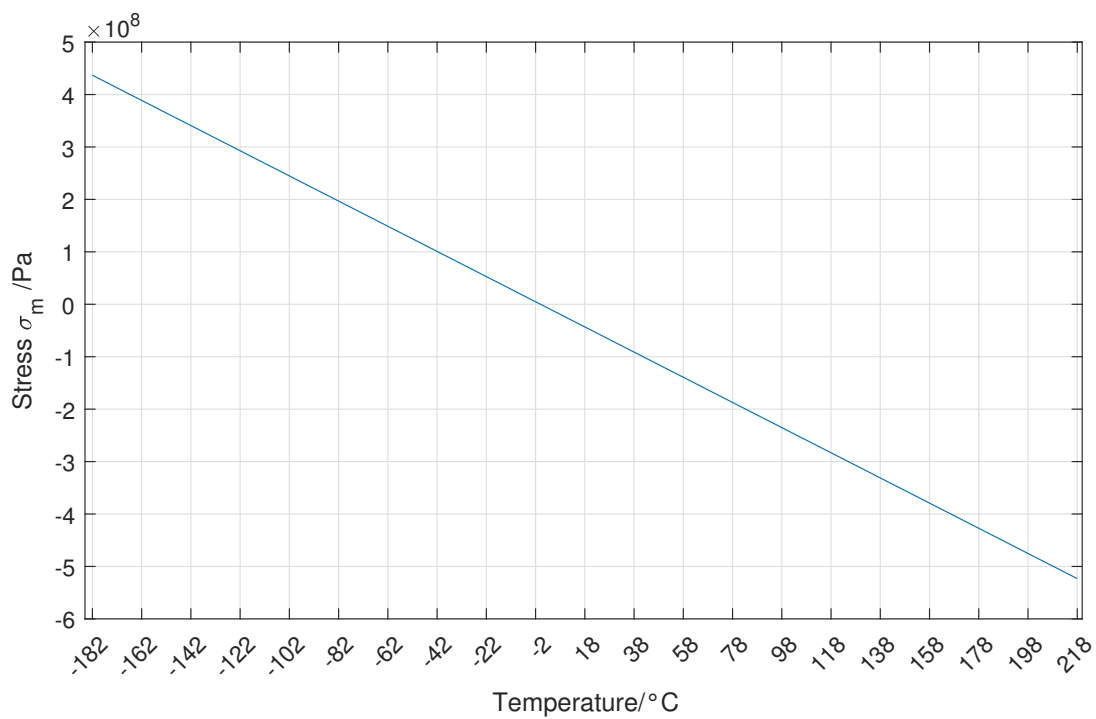
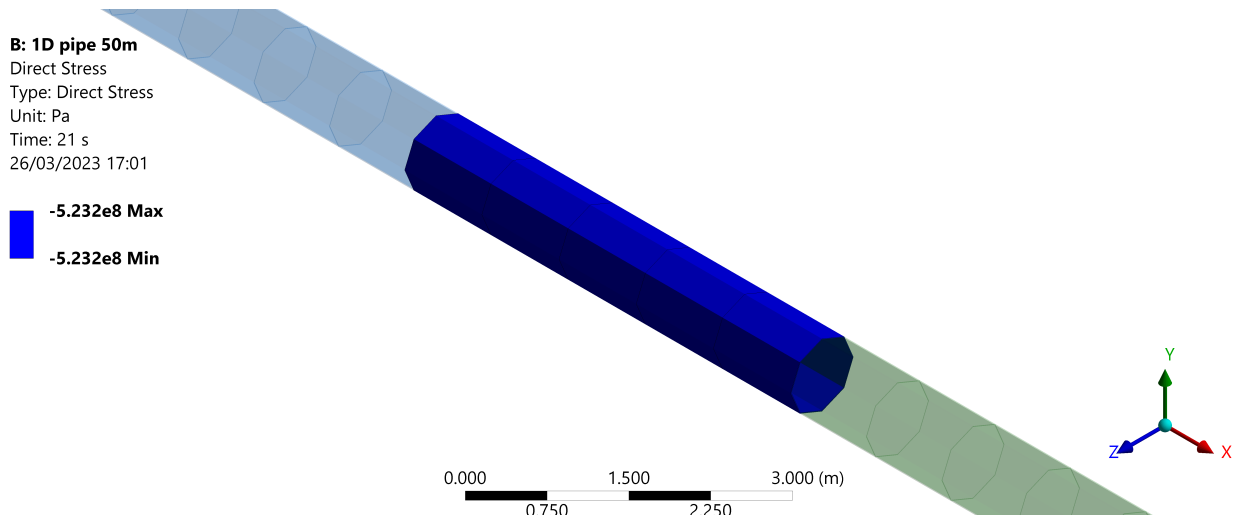
Figure 9: Plot of  $\sigma_m$  in 1D pipe.

Figure 10: 1D pipe at time-step 21, 240 °C, axial stress.

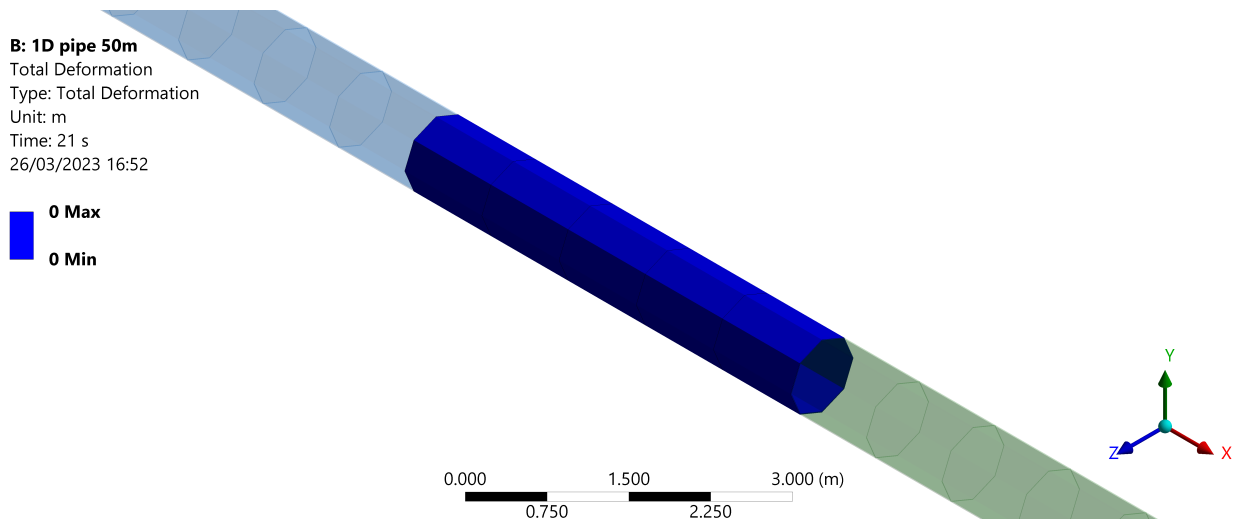


Figure 11: 1D pipe at time-step 21, 240 °C, deformation. Note that there is no deformation.

#### 1.4.2 Comparison against theoretical result and discussion

The theoretical result was calculated using (30). MATLAB was used to plot the results. Figure 12 shows the results from ANSYS and MATLAB plotted on the same graph. The variables used in the equation are the same as the ones used in the 3D analysis, shown in Table 1.

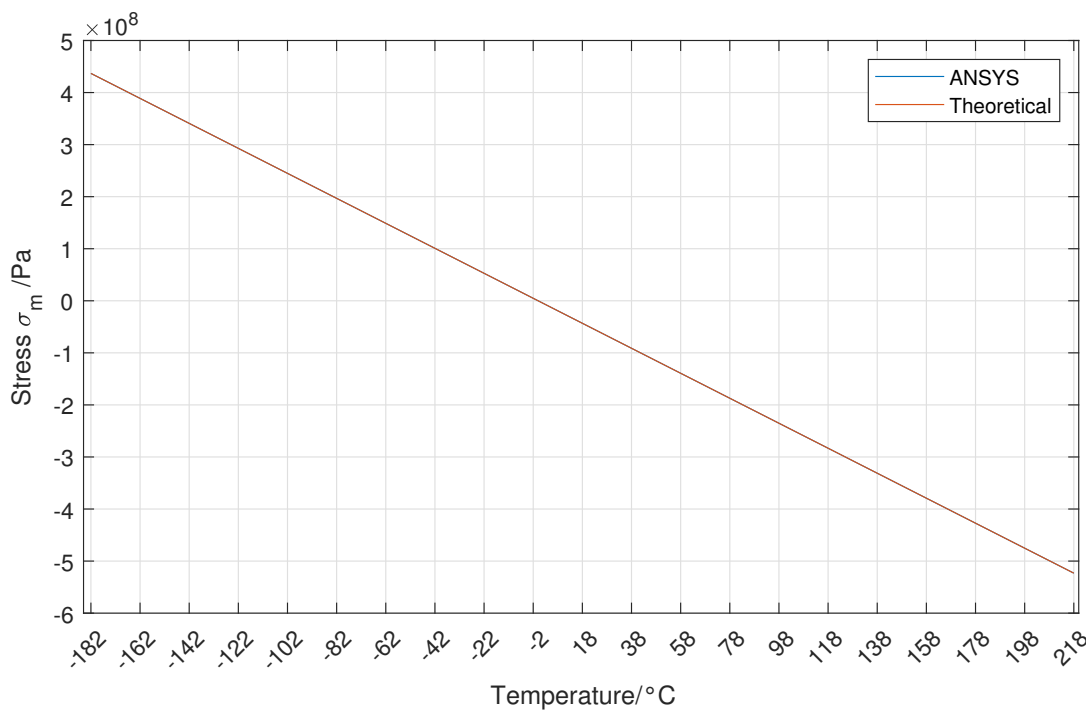


Figure 12: Plot of  $\sigma_m$  in 1D pipe from ANSYS and theoretical calculation.

The results show an identical stress magnitude. An average percentage of difference of 0 % was calculated for the results. As the simulation is utilising a 1D model, it is not accounting for changes in the thickness of the pipe (as this is absent from the simulation), hence, any contribution that may have on the axial stress is not captured in the simulation, giving us an exact result to the theoretical.

## 1.5 Discussion

### 1.5.1 Difference and similarities between results from 1.2, 1.3, 1.4 as pipe slenderness changes

As the slenderness ratio changes ( $L/D_e$ ), the accuracy of both simulations will change. The 1D model may become more accurate as the assumptions made for 1D modelling become more valid. Those assumptions are:

1. The pipe is assumed to be perfectly straight and uniform in diameter
  - This assumption is the same as the one used in our theoretical analysis. However, it must be noted that this would not be the case in any real-world scenario
2. The temperature and thermal expansion of the pipe ('thermal condition' in ANSYS) are assumed to be constant along the length of the pipe
  - This assumption becomes more valid as the length of the pipe increases, since the temperature and thermal expansion are less likely to vary significantly along the length of the pipe in a real-world case
3. There are no axial, bending or torsional loads acting on the pipe
  - As the slenderness increases, the effects of bending, torsion and transverse shear are (relatively) less significant, and the pipe can be better modelled as a 1D structure
4. The material properties of the pipe are assumed to be constant along its length
  - This assumption is the same as that made in the theoretical. As previously noted, this would be impossible to achieve realistically
5. The pipe is assumed to be isotropic

Another point of note is that the 1D simulation is highly dependent on a specific set of boundary and loading conditions. If the boundary/loading conditions were to be made more complex, our model may break down and lose accuracy, regardless of the pipe slenderness.

It may be expected that the 3D model become less accurate as the pipe slenderness changes. Due to the assumptions made in the theoretical analysis, the 3D model better captures the intricacies of the pipe's design, which may contribute to the result. Hence, we may see more deviation in our results as the pipe slenderness changes. The cause of those errors may be:

1. Boundary conditions: the accuracy of the simulation is highly dependent on the accuracy and validity of the boundary conditions applied to the model. As noted previously, the differences between using fixed supports and remote displacement boundary conditions can change our results to a notable degree. As the pipe slenderness changes, it may be increasingly difficult to apply realistic (and hence valid) boundary conditions, leading to inaccuracies
2. Numerical errors: As the pipe slenderness increases, the number of elements required to accurately model the geometry also increases. This can result in numerical errors arising from insufficient element density, if a proper mesh convergence test is not performed
3. Assumptions: while the 3D simulation allows for more complex modelling than the 1D simulation, there are still assumptions made in the modelling process. E.g. the 3D simulation assumes perfect straightness, isotropy, and uniformity in diameter, which is unrealistic. As the pipe becomes longer, small imperfections may become more significant and affect the accuracy of the simulation

In conclusion, the accuracy of simulations of a pipe subjected to temperature changes varies depending on the slenderness ratio ( $L/D_e$ ) and the modelling approach used. The theoretical analysis provides a simplified representation of the problem and makes several assumptions. As the slenderness ratio increases, the 1D modelling approach becomes more valid, since the assumptions made become more accurate. However, this approach still makes some simplifications and may not account for certain effects. The 3D modelling approach provides a more accurate representation of the problem, but as the slenderness ratio increases, the accuracy decreases due

to the increasing complexity and the limitations of the modelling software. Therefore, the choice of modelling approach should be based on the specific problem and the required level of accuracy.

### 1.5.2 Model errors encountered using ANSYS Static Structural model

When using ANSYS static structural to model a pipe under various slenderness ratios, there are several model errors that may occur, resulting in reduced accuracy of the simulation.

As the slenderness of the pipe increases, the accuracy of the 3D model decreases due to the assumption of a constant cross-section. In reality, as the pipe becomes more slender, there may be non-uniform changes in diameter, wall thickness, and even curvature, which the 3D model cannot account for. This leads to errors in the simulation results, such as incorrect stress distributions and deformations.

Increasing the slenderness ratio can lead to a number of errors related to the finite element method (FEM) calculations performed by the software. For example, the number of elements required to discretise the pipe may become too large, resulting in computational inefficiency and increased runtime. This can also lead to the model becoming numerically unstable, as the stiffness matrix may become ill-conditioned due to the high aspect ratio of the elements. Additionally, there may be difficulties in accurately capturing the effects of bending, torsion, and transverse shear forces on the pipe, leading to errors in the stress and strain fields. These errors can be exacerbated by the assumptions made in the 1D modelling approach, such as the assumption of uniform temperature and thermal expansion along the length of the pipe. Finally, the ANSYS static structural model also assumes that there are no axial, bending, or torsional loads acting on the pipe. In reality, the pipe may be subjected to some degree of loading, which can lead to errors in the simulation results.

## 2 Influence of temperature on the response of an expansion loop

### 2.1 Comparison of shape of expansion loop

ANSYS was used to conduct analysis on a 3D expansion loop to determine the shape of the expansion loop at  $T = -160^\circ\text{C}$  and  $T = 240^\circ\text{C}$ . The pipe geometry is shown in Figure 13.

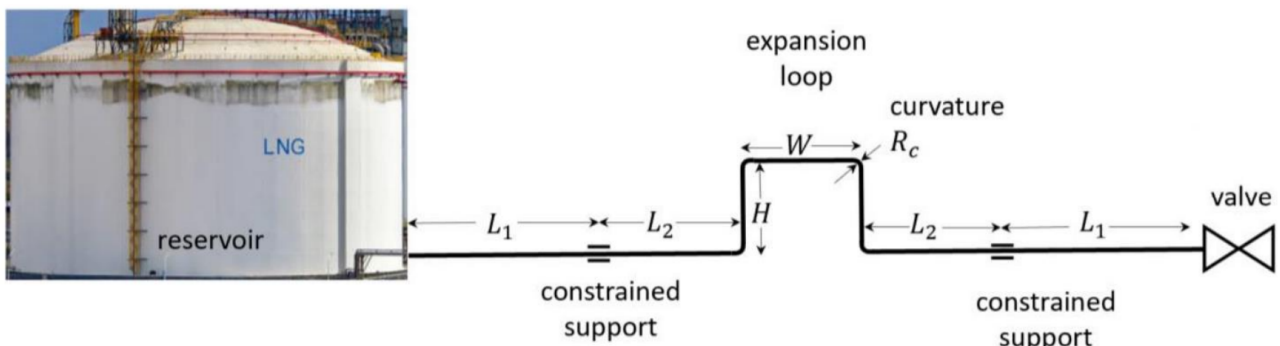


Figure 13: 3D expansion loop geometry.

The geometry was constructed in ANSYS Discovery. ‘Fixed supports’ were used at the ends of the pipe, and ‘displacement’ supports with fixed y and z displacements were added between  $L_1$  and  $L_2$ , to allow the pipe to move axially in the x direction. The simulation utilised 21 steps and a thermal condition spanning the temperature range was added. Figure 14 shows the deformation at  $T = -160^\circ\text{C}$  and Figure 15 shows the deformation at  $T = 240^\circ\text{C}$ .

**C: 3D expansion loop**

Total Deformation  
Type: Total Deformation  
Unit: m  
Time: 1 s  
27/03/2023 01:20

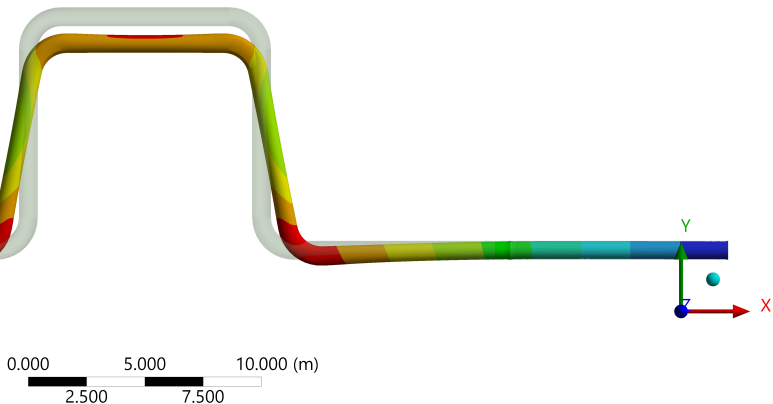
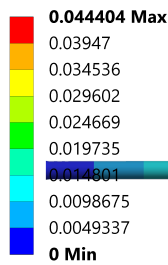


Figure 14: 3D expansion loop deformation in comparison to undeformed case at  $T = -160 \text{ }^{\circ}\text{C}$ .

At  $T = -160 \text{ }^{\circ}\text{C}$ , we see that the expansion loop has contracted and caused the U shape of the loop to be pushed outwards. The bottom pipe bends have deformed the most and have become more obtuse (from  $90^\circ$ ). Sections  $L_2$  has been pushed downwards as a result of the contraction from  $L_1$  and the constraints applied, as has section  $W$ . Sections  $H$  have been rotated as a result of the contraction.

**C: 3D expansion loop**

Total Deformation  
Type: Total Deformation  
Unit: m  
Time: 2 s  
27/03/2023 01:20

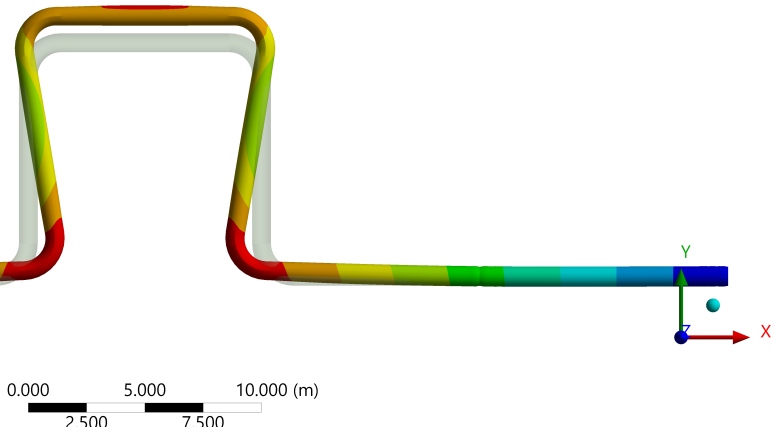
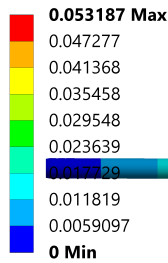


Figure 15: 3D expansion loop deformation in comparison to undeformed case at  $T = 240 \text{ }^{\circ}\text{C}$ .

At  $T = 240 \text{ }^{\circ}\text{C}$ , we see that the expansion loop has expanded and caused the U shape of the loop to be pushed inwards. The bottom pipe bends have again deformed the most and have become acute. Sections  $L_2$  have been pushed upwards slightly as a result of the expansion of  $L_1$  and the constraints applied. Section  $W$  has been pushed upward as a result of the expansion and sections  $H$  have been rotated as a result of the expansion.

Thermoelastic stress is dependent on the material's thermal expansion coefficient, which is a measure of how much the material will expand or contract in response to temperature changes. It is also dependent on the magnitude and rate of temperature change (something not captured in ANSYS Static Structural), as well as the geometry and boundary conditions of the material.

If the temperature change is rapid or significant, the resulting thermoelastic stress can be high and potentially cause damage or failure in the material. However, if the temperature change is gradual and within the material's design limits, the resulting thermoelastic stress can be controlled and beneficial for certain applications, such as this.

Understanding thermoelastic stress is crucial for designing materials and structures that can withstand temperature changes and avoid failure due to stress and deformation.

## 2.2 Plot of variation of maximum displacement of pipe bends

The pipe bend surfaces were indexed in the analysis, and the component deformations in the x and y axes were found. The maximum displacements from each time step were plotted in MATLAB. Figures 16, 17 show the deformations in x and y axis respectively.

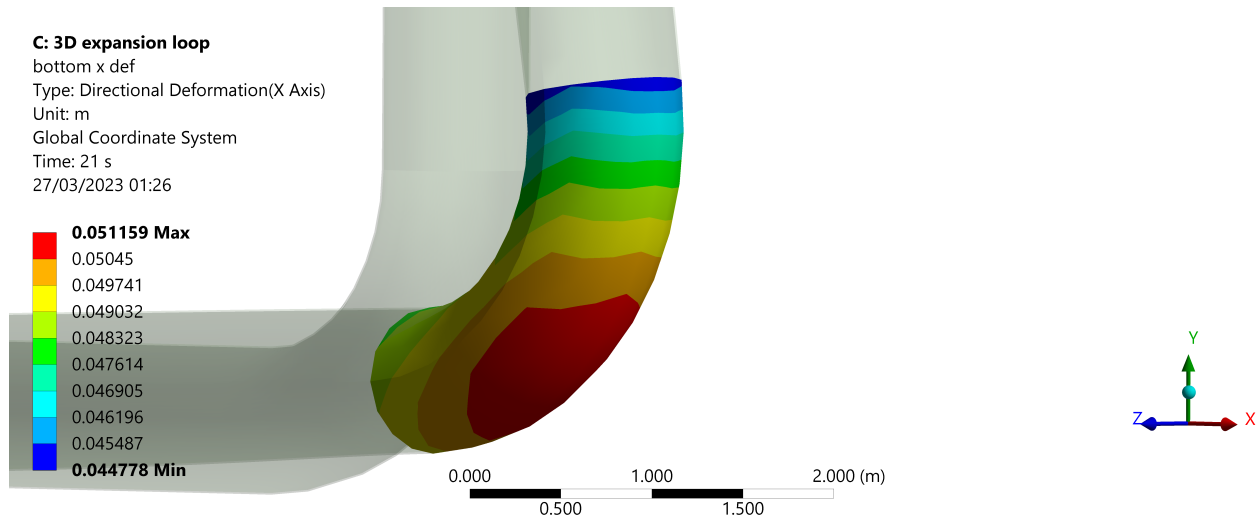


Figure 16: ANSYS maximum deformation in x-axis at time step 21,  $T - T_0 = 218^\circ\text{C}$ , bottom pipe bend.

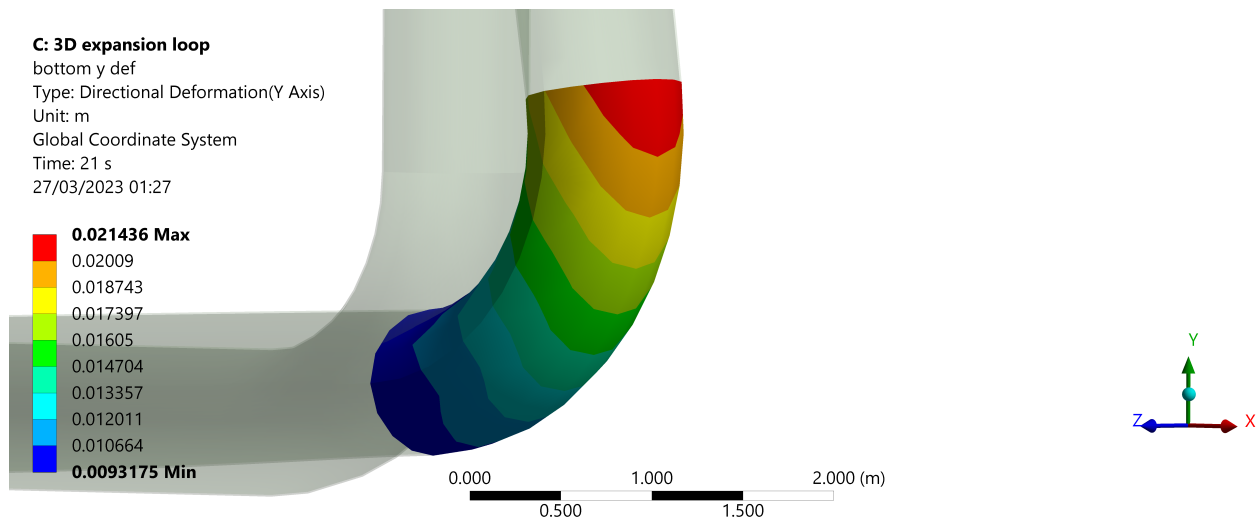


Figure 17: ANSYS maximum deformation in y-axis at time step 21,  $T - T_0 = 218^\circ\text{C}$ , bottom pipe bend.

Figure 18 shows a comparison in the location of the maximum deformation between the first time step and the last. We see that the point of maximum deformation is the apex of the outside bend of the pipe. This appears to be consistent throughout all the time steps in the analysis. Another point of major deformation is the connection point between the bend and the vertical section of the loop. One problem that arises is ANSYS gives us the smallest deformation as maximum for negative results and the largest deformation for positive results. Usually, this is not an issue as we can average between maximum and minimum. However, for the interest in consistency, the node at which maximum displacement occurs in all time steps was selected to index results, to avoid the issue of different parts of the surface being indexed as ‘maximum’ deformation. The node selected for the bottom bend is shown in Figure 19 and a similarly placed node (at the point of maximum deformation) was chosen for the top bend. The results were indexed for one half of the loop (left side), as the loop is symmetrical.

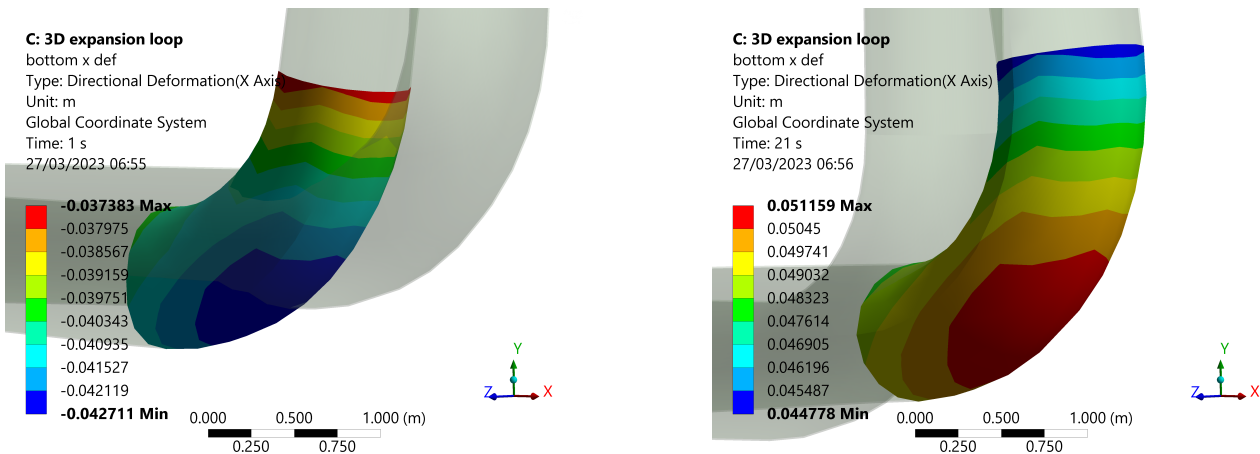


Figure 18: ANSYS maximum deformation in x-axis at time step 1 and 21,  $T - T_0 = -188^\circ\text{C} - 218^\circ\text{C}$ , bottom pipe bend.

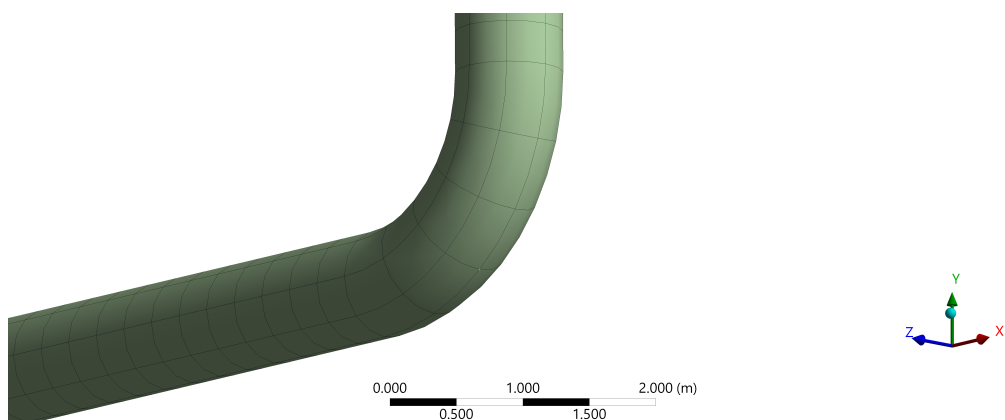


Figure 19: Node selected for pipe bend analysis.

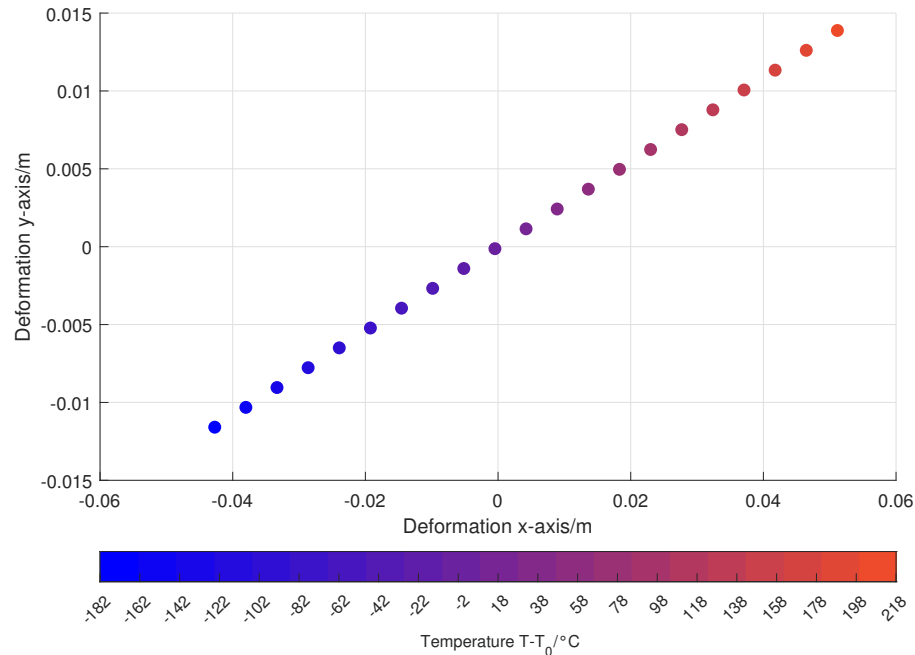


Figure 20: Plot to show maximum displacement of bottom pipe bend at node of maximum displacement.

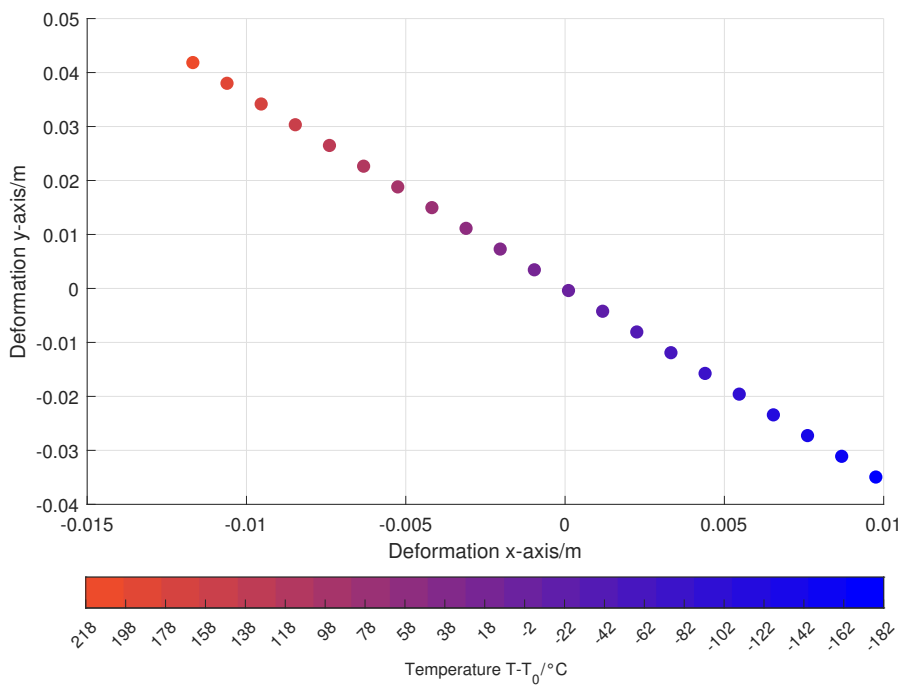


Figure 21: Plot to show maximum displacement of top pipe bend at node of maximum displacement.

The plots show a linear deformation. Note that the deformation in the x-axis is less overall than in the y-axis in Figure 20 (bottom bend) and this is the opposite in Figure 21 (top bend).

### 2.3 Plot of variation of maximum stress of pipe bends

The maximum principal stress was indexed in the results from ANSYS. This was then plotted in Figure 23. The maximum shear stress was also indexed and plotted alongside the maximum principal stress in Figure 24. The results show that the maximum principal stress occurs in the top bend of the pipe on the lateral edges, as shown in Figure 22

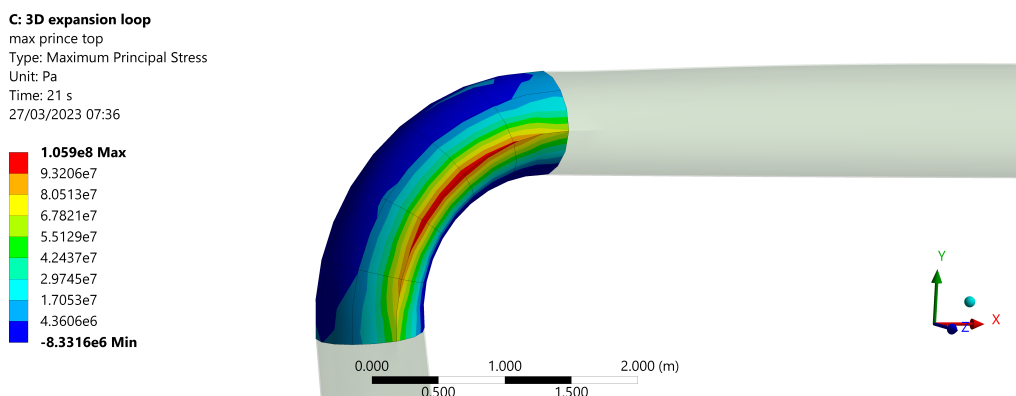


Figure 22: ANSYS maximum principal stress contour plot at time step 21,  $T - T_0 = 218 \text{ } ^\circ\text{C}$ , bottom pipe bend.

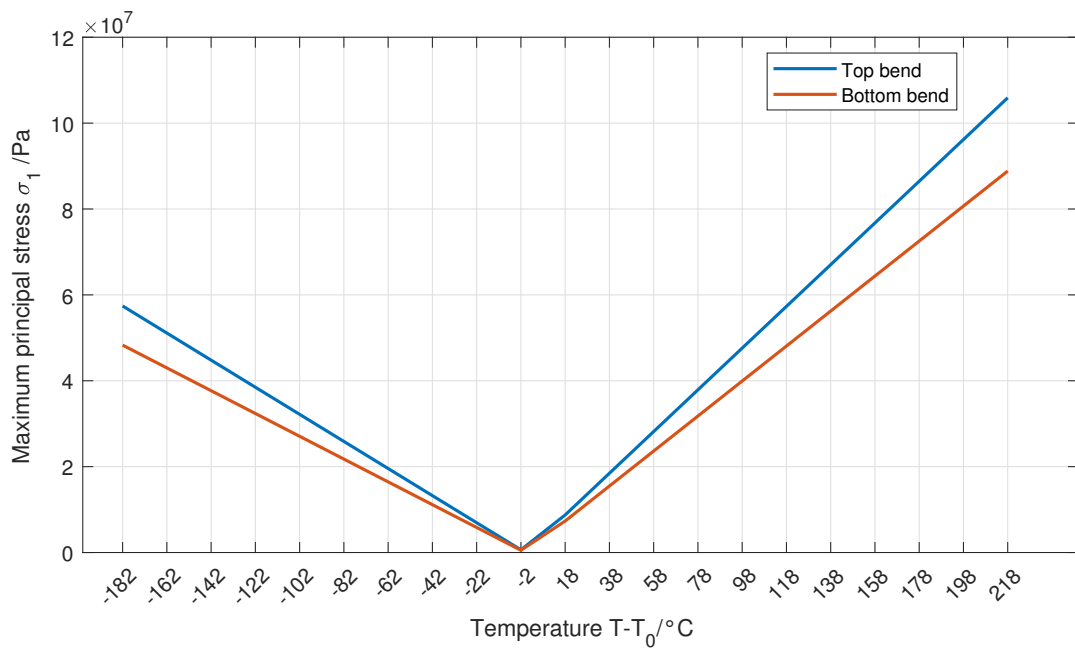
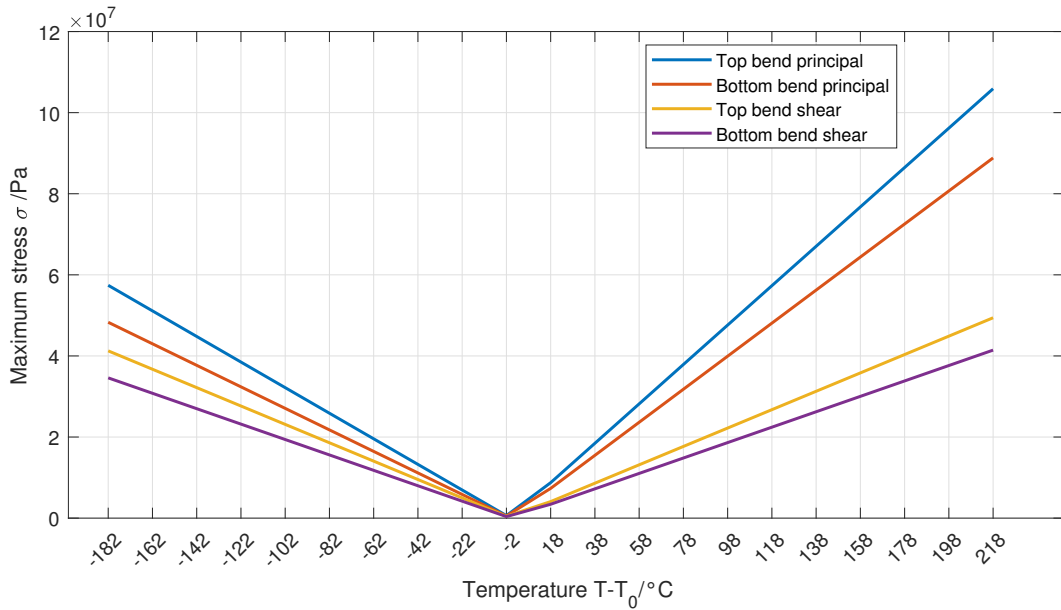
Figure 23: Plot to show maximum principal stress  $\sigma_1$  of pipe bends.

Figure 24: Plot to show maximum principal and shear stress of pipe bends.

## 2.4 Comparison of numerical results

The numerical results from each section show that straight sections of pipe have significantly more stress than those with a loop. We see that in the 3D simulation of a straight pipe, our maximum stress is approximately  $-5 \times 10^8$  Pa. In comparison our 3D expansion loop has a maximum stress of  $1 \times 10^8$  in a comparatively small region at the pipe bend. The rest of the pipe has a much lower stress overall, as can be seen from the 1D simulation; 1 order of magnitude lower approximately. This shows that expansion loops are an effective tool in reducing overall pipe stress over a given span.

The practical implications of including an expansion loop in a pipework design are numerous. The first and major design implication is the extra space required for an expansion loop, requiring much more consideration, especially in complex scenarios with a high density of pipework. This coursework has considered a relatively

simple design for an expansion loop, only extending in-plane. However, expansion loops can take up larger volumes if they are designed with two loops (one extending in-plane and one extending out of plane). Yavuz provides the rationale for design requirements and recommendations for expansion loop designs in the Oil and Gas industry, mentioning that expansion loops extending in all three dimensions prevent possible conflicts to other lines [3]. However, such complexity comes at a cost (in many forms). First, we must consider that more complex loops require more complex supports and these must be modelled beforehand increasing development time and cost. Second, more complex loops require more material and bracing which has a physical and monetary cost associated with it. Third, the maintenance of such a loop must also be considered as more complex piping and bracing requires thorough checks and potentially repairs over the course of its lifetime. Another consideration is the overall pressure drop in the system as a result of the increase in the total length of the pipe. This effect can be mitigated by carefully selecting the length and configuration of the expansion loop, as well as the material properties of the piping and the fluid being transported.

In the UK, all piping must follow a set of codes as outlined by the Health and Safety Executive (HSE). Specifically, the HSE outlines via a Technical Measures Document the specific codes that must be followed for design work involving pipework [4]. ASME B31.3 is the code that outline the design, construction, operation, and maintenance requirements for piping systems, specifically for Process Piping [5]. Other codes of interest are the Pressure Systems Safety Regulations 2000, which outlines general safety regulations around pipework and the California Plumbing Code 2022, which outlines specific geometry and equations for expansion loop design [6, 7].

In ASME B31.3, the maximum allowable stress takes the following form in the thermal expansion case:

$$S = f \left[ \left( \left( \frac{1.25}{E} \right) \times (S_c + S_h) \right) - S_E \right] \quad (31)$$

where  $f$  is the stress range factor,  $E$  is Young's Modulus,  $S_c$  is the basic allowable stress at minimum metal temperature,  $S_h$  is the basic allowable stress at maximum metal temperature and  $S_E$  is the code stress.  $S_E$  is defined as:

$$S_E = \sqrt{S_b^2 + 4S_t^2} \quad (32)$$

where  $S_b$  is the bending stress and  $S_t$  is the torsional stress. To make a comparison, the California Plumbing codes utilise a different methodology, giving specifications to the lengths of different parts of the expansion loop. The California Plumbing code state that the minimum length of expansion arms  $LB$  shall be calculated using the following equation:

$$LB = C \times \sqrt{D \times \Delta L} \quad (33)$$

where  $C$  is the material constant,  $D$  is the nominal outside diameter of tubing and  $\Delta L$  is the thermal expansion length. Hence:

$$LB = W + (2 \times H) \quad (34)$$

where  $W = LB/5$  is the length of the top part of the loop, and  $H = 2W$  is the length of the vertical sections of the loop (as specified in the earlier geometry used for expansion loop analysis).

Shehadeh *et al* conducts 'an optimization analysis concerning the expansion loop dimensions and the number of supports without compromising on the safety of piping. The design approach is conducted as per the guidelines of ASME B31.3 (Process Piping) code.' The analysis results show that through a physics based approach, expansion loops can be well designed to minimise material and cost, whilst adhering to ASME B31 codes, rather than through empirical means, which is the norm in industry [8].

The practical implications of including an expansion loop in a pipework design are significant and require careful consideration of various factors, including material selection, installation and maintenance, system compatibility, and cost considerations. However, by following industry standards and best practices, the inclusion of this expansion loop can greatly improve the reliability and longevity of the piping system, making it a worthwhile investment in many cases.

## 2.5 1D pipe model and consequences of increasing length L1 and effect on maximum pipe stress

ANSYS was used to construct two expansion loops with  $L_1 = 10\text{ m}$  and  $L_1 = 50\text{ m}$ . The results are shown in the following Figures.

**D: 1D expansion loop**  
 Maximum Combined Stress  
 Type: Maximum Combined Stress  
 Unit: Pa  
 Time: 1 s  
 27/03/2023 05:20

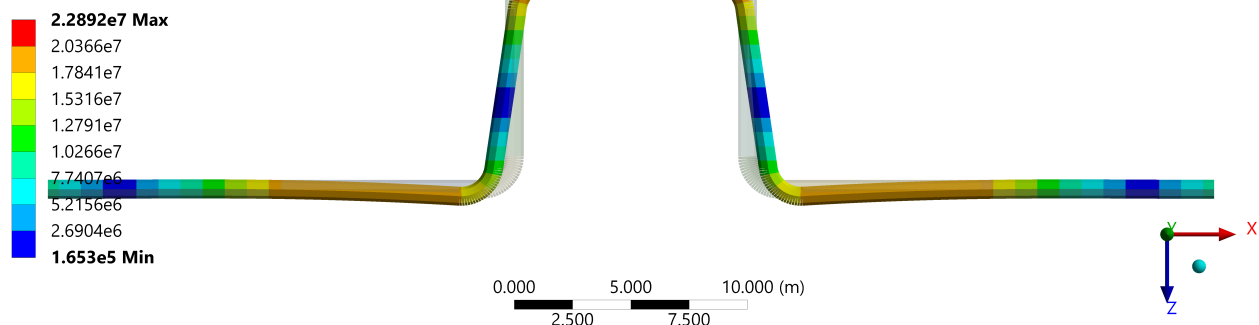


Figure 25: ANSYS results from 1D expansion loop  $L_1 = 10\text{ m}$ , time step 1,  $T = -160\text{ }^\circ\text{C}$ , maximum combined stress.

**D: 1D expansion loop**  
 Maximum Combined Stress  
 Type: Maximum Combined Stress  
 Unit: Pa  
 Time: 21 s  
 27/03/2023 05:20

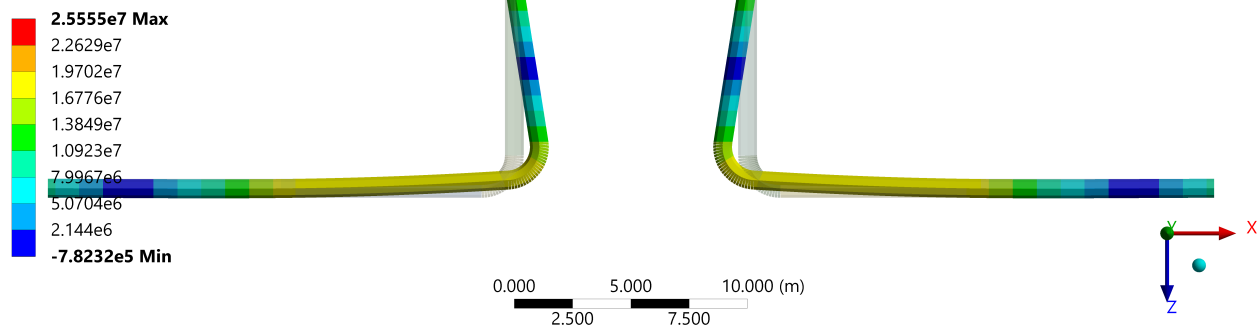


Figure 26: ANSYS results from 1D expansion loop  $L_1 = 10\text{ m}$ , time step 21,  $T = 240\text{ }^\circ\text{C}$ , maximum combined stress.

**F: Copy of 1D expansion loop**

Maximum Combined Stress  
 Type: Maximum Combined Stress  
 Unit: Pa  
 Time: 1 s  
 27/03/2023 05:21

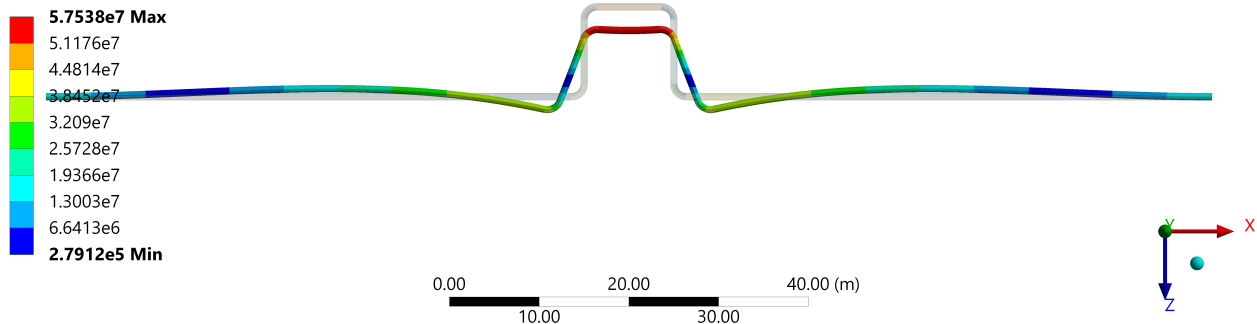


Figure 27: ANSYS results from 1D expansion loop  $L_1 = 50$  m, time step 1,  $T = -160$  °C, maximum combined stress.

**F: Copy of 1D expansion loop**

Maximum Combined Stress  
 Type: Maximum Combined Stress  
 Unit: Pa  
 Time: 21 s  
 27/03/2023 05:22

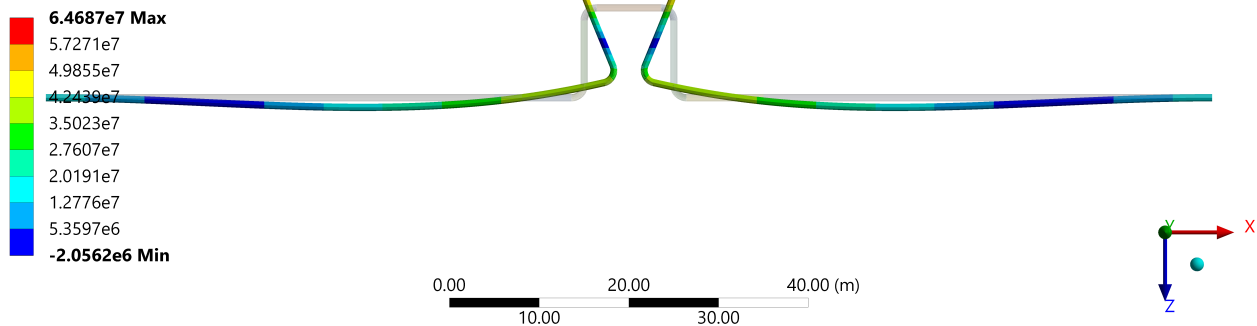


Figure 28: ANSYS results from 1D expansion loop  $L_1 = 50$  m, time step 21,  $T = 240$  °C, maximum combined stress.

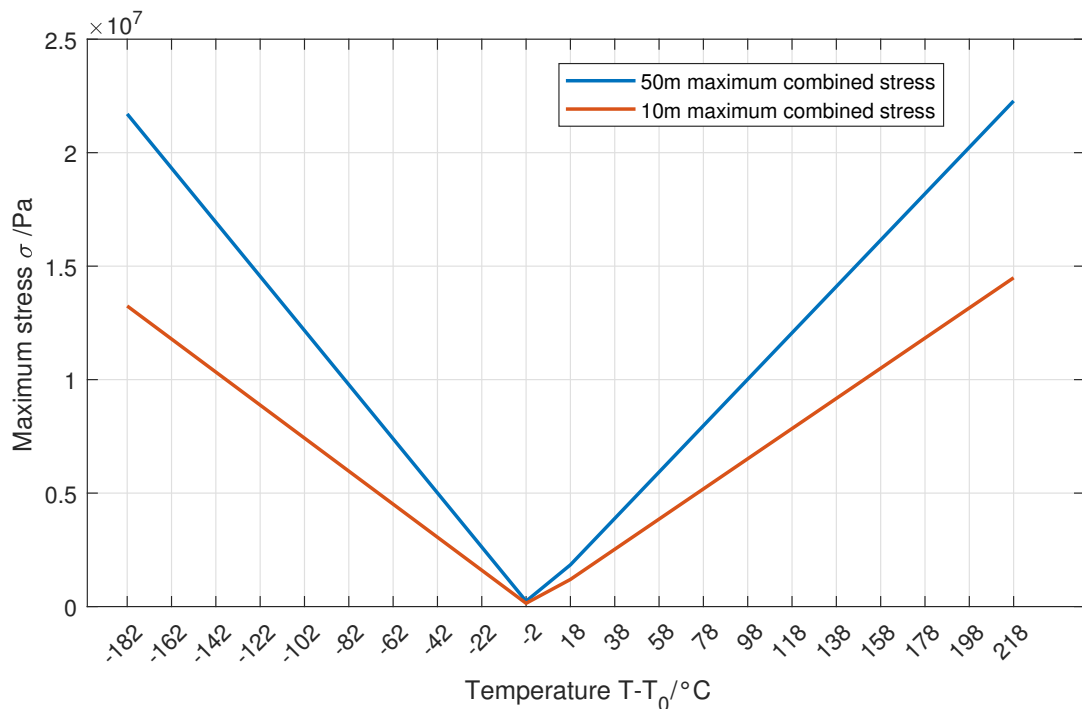


Figure 29: Maximum combined stress of  $L_1$  50 m and 10 m expansion loops.

The results show that as  $L_1$  increases, the maximum combined stress increases in all cases. This is due to the fact that there is more material that is subject to contraction/expansion. Due to the constraint at the boundary between  $L_1$  and  $L_2$ , we see higher stresses due to higher deformation in the loop.

Increasing the size of  $L_1$  may also require changes to the design of the supports used to hold the loop in place. For larger loops, additional supports may be required to ensure that the loop remains stable and does not experience excessive stress, deflection or deformation from the thermal expansion of the material. This can also have implications for the overall safety and reliability of the system, and may require additional design considerations to ensure that the system remains within safe operating limits.

## References

- [1] A.S. Usmani, J.M. Rotter, S. Lamont, A.M. Sanad, and M. Gillie. Fundamental principles of structural behaviour under thermal effects. *Fire Safety Journal*, 36(8):721–744, 2001. ISSN 0379-7112. URL <https://www.sciencedirect.com/science/article/pii/S0379711201000376>. Response of Composite Steel Framed Structures to Fire.
- [2] ANSYS Inc. Ansys workbench products release notes. online, 2005. URL <https://kashanu.ac.ir/Files/Content/ANSYS%20Workbench.pdf>. Accessed 20/03/2023.
- [3] Bekir Yavuz. Implementation of expansion loops, 10 2015.
- [4] UK Health and Safety Executive. Design codes - pipework. online, 2023. URL <https://www.hse.gov.uk/comah/sragtech/techmeaspipework.htm>. Accessed 27/03/2023.
- [5] American Society of Mechanical Engineers. Asme b31.3: Process piping, 2018. URL <https://www.asme.org/codes-standards/find-codes-standards/b31-3-process-piping>. Accessed 27/03/2023.
- [6] UK Health and Safety Executive. Pressure systems safety regulations 2000. approved code of practice and guidance on regulations. online, 2000. URL <https://www.hse.gov.uk/pubns/books/l122.htm>. Accessed 27/03/2023.
- [7] State of California. California plumbing code 2022. online, 2022. URL <https://up.codes/viewer/california/ca-plumbing-code-2022/chapter/I/installation-standards#6.4>. Accessed 27/03/2023.
- [8] Bahaa Shehadeh, Shivakumar Ranganathan, and Farid Abed. Optimization of piping expansion loops using asme b31.3. *Proceedings of the Institution of Mechanical Engineers, Part E: Journal of Process Mechanical Engineering*, 230, 01 2014. doi: 10.1177/0954408914532808.

## A Code for Part 1C

```
1 %% HD
2
3 clc
4 clear
5 close all
6
7 %% import data
8
9 ansys = readmatrix('avg-stress-x-direction-3D.txt');
10 % step | time | min Pa | max Pa | avg Pa
11 ansys(1,:) = [];
12
13 %% theoretical result
14
15 % constants
16
17 alpha = 1.196e-05; %ansys
18 E = 2.1e11; %ansys
19 intTempPipe = 22; %degC
20 T = linspace(-160,240,21)'; %degC
21 stressxx = -alpha*E*(T - intTempPipe);
22
23 T2 = linspace(-160-22,240-22,21)';
24
25 %% plot
26
27 plot(T2,ansys(:,5),T2,stressxx)
28 grid on
29 xlabel(['Temperature T-T_0/' char(176) 'C']);
30 ylabel('Stress \sigma_m /Pa');
31 xlim([-185,220])
32 xticks(-160-22:20:240-22)
33 ylim([-6e8,5e8])
34 yticks(-6e8:1e8:5e8)
35 legend('ANSYS','Theoretical')
36
37 %% perc diff
38
39 percDiff = (ansys(:,5)-stressxx)./stressxx;
40 percDiffAvg = sum(abs(percDiff))/21;
```

## B Code for Part 1D

```
1 %% HD
2
3 clc
4 clear
5 close all
6
7 %% import data
8
9 ansys = readmatrix('avg-stress-x-direction-1d-split.txt');
10 ansys3d = readmatrix('avg-stress-x-direction-3D-sameMaterial');
11 % step | time | min Pa | max Pa | avg Pa
12 ansys(1,:) = [];
13 ansys3d(1,:) = [];
14
15 %% theoretical result
16
17 % constants
18
19 alpha = 1.2e-05 ; %ansys
20 E = 2e11; %ansys
21 intTempPipe = 22; %degC
22 T = linspace(-160,240,21)'; %degC
23 stressxx = -alpha*E*(T - intTempPipe);
24
25 T2 = linspace(-160-22,240-22,21)';
26
27 %% plot
28
29 plot(T2,ansys(:,4),T2,stressxx)
30 grid on
31 xlabel(['Temperature/' char(176) 'C']);
32 ylabel('Stress \sigma_m /Pa');
33 xlim([-185,220])
34 xticks(-160-22:20:240-22)
35 ylim([-6e8,5e8])
36 yticks(-6e8:1e8:5e8)
37 legend('ANSYS','Theoretical')
38
39 %% perc diff
40
41 percDiff = (ansys(:,4)-stressxx)./stressxx;
42 percDiffAvg = sum(abs(percDiff))/21;
```

## C Code for Part 2B

```
1 %% HD
2
3 clc
4 clear
5 close all
6
7 %% import data
8
9 topx = readmatrix('top-x-displacement-nodal.txt');
10 topy = readmatrix('top-y-displacement-nodal.txt');
11 botx = readmatrix('bot-x-displacement-nodal.txt');
12 boty = readmatrix('bot-y-displacement-nodal.txt');
13 % step | time | min m | max m | avg m
14
15 topx(1,:) = [];
16 topy(1,:) = [];
17 botx(1,:) = [];
18 boty(1,:) = [];
19
20 %% plots
21 % setup
22 sz = 50;
23 c = linspace(-160-22,240-22,21);
24 darkblue = [0,0,255];
25 brightred = [238,75,43];
26 colour = [linspace(darkblue(1,1),brightred(1,1),21)',...
27     linspace(darkblue(1,2),brightred(1,2),21)',...
28     linspace(darkblue(1,3),brightred(1,3),21)']/256;
29 % x-y deformation top bend
30 scatter(topx(:,5),topy(:,5),sz,c,'filled');
31 % settings
32 colormap(colour);
33 colorHandle = colorbar();
34 a=colorbar;
35 a.Location = 'southoutside';
36 a.Direction = 'reverse';
37 a.Label.String = ['Temperature T-T_0/' char(176) 'C'];
38 hColourbar.Label.Position(1) = 50;
39 a.Ticks = c;
40 a.TickLabels = num2cell(c);
41 grid on
42 xlabel('Deformation x-axis/m');
43 ylabel('Deformation y-axis/m');
44
45 %
46 plot(topx(:,4),topy(:,4))
47 axis equal
48 xlim([-10e-3,10e-3])
49 ylim([-0.05,0.05])
50 %}
```

## D Code for Part 2C

```
1 %% HD
2
3 clc
4 clear
5 close all
6
7 %% import data
8
9 topStress = readmatrix('max-principal-stress-top.txt');
10 topShear = readmatrix('max-principal-shear-stress-top.txt');
11 botStress = readmatrix('max-principal-stress-bot.txt');
12 botShear = readmatrix('max-principal-shear-stress-bot.txt');
13 % step | time | min Pa | max Pa | avg Pa
14
15 topStress(1,:) = [];
16 topShear(1,:) = [];
17 botStress(1,:) = [];
18 botShear(1,:) = [];
19
20 T = linspace(-160-22,240-22,21);
21
22 %% plots
23
24 plot(T,topStress(:,4), T,botStress(:,4), T,topShear(:,4),
      T,botShear(:,4),'LineWidth',1.5)
25 grid on
26 xlabel(['Temperature T-T_0/' char(176) 'C']);
27 ylabel('Maximum stress \sigma /Pa');
28 xticks(-160-22:20:240-22)
29 legend('Top bend principal','Bottom bend principal','Top bend
      shear','Bottom bend shear')
```

## E Code for Part 2E

```
1 %% HD
2
3 clc
4 clear
5 close all
6
7 %% import data
8
9 L50m = readmatrix('maximumStress-50m.txt');
10 L10m = readmatrix('maximumStress-10m.txt');
11 L50mBend = readmatrix('deformationL1-50m-bottom-pipe-bend');
12 L10mBend = readmatrix('deformationL1-10m-bottom-pipe-bend');
13
14 L50m(1,:) = [];
15 L10m(1,:) = [];
16 L50mBend(1,:) = [];
17 L10mBend(1,:) = [];
18
19 T = linspace(-160-22,240-22,21);
20
21 %% plots
22
23 plot(T,L50m(:,5), T,L10m(:,5), 'LineWidth',1.5)
24 grid on
25 xlabel(['Temperature T-T_0/' char(176) 'C']);
26 ylabel('Maximum stress \sigma /Pa');
27 xticks(-160-22:20:240-22)
28 legend('50m maximum combined stress','10m maximum combined stress')
```